Chapter 33
Precise Point Positioning Using GPS and Compass Observations

Wei Li, Peter Teunissen, Baocheng Zhang and Sandra Verhagen

Abstract The Compass Navigation Satellite system, which currently provides more than 12 satellites with three carrier signals, already satisfies the requirement of stand-alone positioning in the Asia–Pacific regional area. First an initial introduction and performance assessment of dual-frequency un-differenced precise point positioning (PPP) for GPS and Compass is presented, the results of which indicate that centimeter-level positioning accuracy of Compass-PPP is comparable to that of GPS-PPP. Then the combined GPS + Compass dual-frequency PPP model is introduced, followed by a numerical performance analysis and comparison with single GNSS-PPP. The results show that the combined GPS + Compass PPP can shorten the convergence time, but not necessarily improve positioning results by much if the satellites of the single GNSS system already have a good receiver-satellite geometry.

Keywords GPS · Compass · GPS + Compass, PPP · Dual and triple-frequency GNSS

W. Li (✉)
School of Geodesy and Geomatics, Wuhan University, Wuhan, China
e-mail: wewelee_c@whu.edu.cn

W. Li
Chinese Academy of Surveying and Mapping, Beijing, China

P. Teunissen · B. Zhang
GNSS Research Centre, Department of Spatial Sciences, Curtin University, Perth, Australia
e-mail: P.Teunissen@curtin.edu.au

S. Verhagen
Department of Remote Sensing and Geoscience, Delft University of Technology, Delft, The Netherlands

J. Sun et al. (eds.), *China Satellite Navigation Conference (CSNC) 2013 Proceedings*, Lecture Notes in Electrical Engineering 244, DOI: 10.1007/978-3-642-37404-3_33,

33.1 Introduction

The Compass Navigation Satellite System is a global navigation satellite system, which is independently deployed and operated by China and still in development. Currently, Compass system consists of fifteen operational satellites transmitting navigation signals at three frequency bands (B1, B2, B3), including five operational Geostationary Orbit (GEO) satellites, five Inclined Geosynchronous Orbit (IGSO) satellites, and five Medium Earth Orbit (MEO) satellites. This enables Compass system to provide navigation service in the Asia–Pacific regional area; by 2020, a global navigation service will be achieved eventually. Worldwide users will be able to have access to services of Compass for positioning, navigation and timing (PNT), and also take advantage of multi-frequency observations from multi-GNSS systems to greatly enhance observation redundancy and the navigation performance [16].

With the increasing development of Compass system, it draws enormous interest and attention of the scientific community. Based on simulated data, Chen et al. [3] and Yang et al. [16] pointed out the contribution of Compass to user's PNT by analysis of visible satellites and dilution of precision (DOP) values. Absolute and relative positioning tests were also performed using simulated Compass observations ([1, 2]). Nadarajah et al. [10, 11] used multiple GNSS antennas mounted on a platform to determine the attitude precisely, with the constrained Least-squares Ambiguity Decorrelation Adjustment (C-LAMBDA) method. They demonstrated this method with real Compass data and quantify the improved availability, reliability, and accuracy of attitude determination using the combined GPS and Compass constellations. Since the Compass navigation message has not yet been publicly released, some community have estimated the orbit and clock of Compass GEO and IGSO satellites based on a network of Compass-capable tracking stations. For example, Steigenberger et al. [15] utilized the dual-frequency GPS (L1 and L2) and Compass (B1 and B2) data from the IGS Multi-GNSS Experiment (MGEX) and the Cooperative Network for GIOVE Observation (CONGO) to estimate the orbit and clock errors of Compass GEO and IGSO satellites, with the orbit quality at meter level for GEO satellites and one to two decimeter level for IGSO satellites. Shi et al. [13] from Wuhan University determined the precise orbit of Compass satellites, with the radial accuracy better than 10 cm. These two communities also pointed out that higher accuracy orbit and clock of Compass satellites can be achieved by denser distributed tracking stations.

Along with the accomplishing of regional Compass system, investigations have focused on positioning performance using real observations mostly. Shi et al. [13, 14] showed that an accuracy of 20 m can be achieved for Compass standalone positioning; in short baseline experiment, the precision of Compass-only relative positioning are 2–4 cm; and the combined GPS + Compass solutions have improved the positioning by at least 20 % compared with GPS-only solutions. Based on achieved orbit and clock products, static PPP and kinematic RTK can also achieve centimeter level and 5–10 cm respectively. Steigenberger et al. [15]

also tested the Compass PPP performance and compared it with GPS PPP in the aspect of positioning and zenith wet delays (ZWD) solutions. Montenbruck et al. [8, 9] demonstrated the high level of stability for the Compass inter-frequency carrier phase biases, and verified the tripe-frequency relative positioning with real Compass data.

PPP is an attractive positioning technique with a high accuracy using a standalone GNSS receiver, and GPS dual-frequency PPP has been an active research topic over the past decade. It is well known that static GPS-PPP is capable of providing millimeter to centimeter positioning accuracy using daily observations [7, 17]. Based on the post-processing Compass orbit and clock products from Steigenberger et al. [15], this contribution aims at showing an initial result of Compass-PPP using daily dual observations, and comparing the performance with dual-frequency GPS-PPP and combined GPS + Compass PPP. In the following sections, the un-differenced PPP algorithm for dual-frequency single and two GNSS systems is presented. Numerical results of Compass-PPP and combined GPS + Compass PPP are firstly reported and discussed.

33.2 Dual-Frequency PPP Algorithms

In the un-differenced PPP algorithm, the original GNSS code and phase observables are adopted; and LOS ionospheric delays are regarded as estimate parameters together with position, receiver clock error, zenith tropospheric delays and ambiguity. In this section, dual-frequency PPP algorithms for single and two GNSSs are both presented, including the functional and stochastic models.

33.2.1 Dual-Frequency PPP

The dual-frequency GNSS code and carrier-phase observation equations can be expressed as:

$$\begin{aligned} p^s_{r,j} &= \rho^s_r + dt_r - dt^s + T^s_r + \mu_j \cdot I^s_{r,1} + b_{r,j} - b^s_j + \varepsilon_p \\ \phi^s_{r,j} &= \rho^s_r + dt_r - dt^s + T^s_r - \mu_j \cdot I^s_{r,1} + \lambda_j \cdot M^s_{r,j} + \varepsilon_\phi \end{aligned} \tag{33.1}$$

where $p^s_{r,j}$, $\phi^s_{r,j}$ denote the code and phase observables from satellite s to receiver r on frequency j. ρ^s_r is the geometric range between satellite and receiver antennas; dt_r and dt^s refer to the receiver and satellite clock errors; T^s_r denotes the tropospheric delays; b^s_j and $b_{r,j}$ are the satellite and receiver code instrumental delays due to the transmitting and receiving hardware; $I^s_{r,1} = 40.28/f_1^2 \cdot sTEC$ is the ionospheric delay on GNSS group signal propagation at frequency f_1, $sTEC$ is the slant total integrated electron content; $\mu_j = \lambda_j^2/\lambda_1^2$, describes the dispersive

ionospheric effect, λ_j is the wavelength at frequency j; $M^s_{r,j}$ is the carrier-phase ambiguity including satellite and receiver phase instrumental delays and initial phase bias; ε_p and ε_ϕ refer to observational noise and multipath effects.

The precise satellite clock products from IGS or other organization, which always refer to ionosphere-free code and phase combinations, can be written as [5, 6]:

$$dt^s_I = dt^s + b^s_{IF} \tag{33.2}$$

where dt^s and dt^s_I denote truth and published values, the precise clock values used in this paper are from IGS and Technical University Munich (TUM, Munich, Germany) for GPS and Compass satellites respectively. $b^s_{IF} = \alpha_2 \cdot b^s_1 - \alpha_1 \cdot b^s_2$ denote the ionosphere-free combination of b^s_1 and b^s_2, $\alpha_j = \mu_j/(\mu_2 - 1)$. When the precise products are utilized, an additional combination of b^s_1 and b^s_2 is introduced to both observation equations, Eq. (33.1) can be written as:

$$\begin{aligned} p^s_{r,j} &= \rho^s_r + dt_r - dt^s_I + T^s_r + \mu_j \cdot I^s_{r,1} + b_{r,IF} + \alpha_j \cdot (B_r - B^s) + \varepsilon_p \\ \phi^s_{r,j} &= \rho^s_r + dt_r - dt^s_I + T^s_r - \mu_j \cdot I^s_{r,1} + \lambda_j \cdot M^s_{r,j} + b^s_{IF} + \varepsilon_\phi \end{aligned} \tag{33.3}$$

Similarly, $b_{r,IF} = \alpha_2 \cdot b_{r,1} - \alpha_1 \cdot b_{r,2}$ denote the ionosphere-free combination of $b_{r,1}$ and $b_{r,2}$, $B^s = b^s_2 - b^s_1$ and $B_r = b_{r,2} - b_{r,1}$ are differential code biases (DCBs) for each satellite and receiver respectively. The above-mentioned code biases can be absorbed in receiver clock, ionospheric delays and phase ambiguity, with the satellite positions X_s fixed, Eq. (33.3) can be linearized near the approximate receiver position X^0_r and the full-rank observation equations can be expressed as:

$$\begin{aligned} \Delta p^s_{r,j} &= -\mathbf{\mu}^s_r \cdot \Delta r + m^s_r \cdot \tau_r + dt^b_r + \mu_j \cdot I^{s,b}_{r,1} + \varepsilon_p \\ \Delta \phi^s_{r,j} &= -\mathbf{\mu}^s_r \cdot \Delta r + m^s_r \cdot \tau_r + dt^b_r - \mu_j \cdot I^{s,b}_{r,1} + \lambda_j \cdot M^{s,b}_{r,j} + \varepsilon_\phi \end{aligned} \tag{33.4}$$

where $\Delta p^s_{r,j}$ and $\Delta \phi^s_{r,j}$ denote the observed minus calculated observations for the code and carrier-phase, for which some systematic errors, satellite clock errors, and dry tropospheric delays, have been a priori corrected; $\mathbf{\mu}^s_r$ is the unit direction vector from receiver r to satellite s; and Δr denotes the three-dimensional increments of X^0_r. m^s_r and τ_r are wet tropospheric mapping function and the remaining wet zenith tropospheric delay. dt^b_r, $I^{s,b}_{r,1}$ and $M^{s,b}_r$ are the estimable receiver clock error, ionospheric delays and carrier-phase ambiguities biased by $b_{r,j}, b^s_j$, which are:

$$dt^b_r = dt_r + b_{r,IF} \tag{33.5}$$

$$I^{s,b}_{r,1} = I^s_{r,1} + \alpha_1 \cdot (B_r - B^s) \tag{33.6}$$

$$\lambda_j \cdot M^{s,b}_{r,j} = \lambda_j \cdot M^s_{r,j} - b_{r,IF} + b^s_{IF} + \alpha_j \cdot (B_r - B^s) \tag{33.7}$$

Assuming m satellites were simultaneously tracked by receiver r, then by incorporating the linearized equations (as Eq. 33.4) for all satellites, the following compact form of the observation equations can be formed:

$$\underset{4m\times 1}{y} = \underset{4m\times(3m+5)}{A} \cdot \underset{(m+5)\times 1}{x} + \underset{4m\times 1}{\varepsilon_y},\ \varepsilon_y \sim N(0, Q_{yy}) \tag{33.8}$$

$$x = [\Delta r_r, \tau_r, dt_r^b, I_{r,1}^{s,b}, M_r^{s,b}]^T \tag{33.9}$$

The unknown vector in the PPP includes three position coordinate parameters, a wet zenith tropospheric delay parameter τ_r, a receive clock correction parameter dt_r^b, slant ionospheric delays at L_1 $I_{r,1}^{s,b}$, and float ambiguity terms $M_r^{s,b}$ at each frequency, where $s = 1 \cdots m$. The quantity Q_{yy} takes the form of a diagonal matrix with its diagonal elements $Q_{ii} = \sigma_0^2 / \sin^2(E_r^s)$, E_r^s is the elevation angle of each satellite and σ_0 is the standard deviation of the GNSS observation at zenith.

33.2.2 Dual-Frequency Combined PPP

Based on Eq. (33.4), the linearized equation can be obtained after applying the GPS and Compass precise orbit and clock corrections. A systematic time difference between GPS and Compass time system is existed, that is $dt_c = dt_G + dt_{sys}$. The estimable clock corrections can be written as:

$$dt_r^{C,b} = dt_r^{G,b} + dt_{sys}^b \tag{33.10}$$

where $dt_{sys}^b = dt_{sys} + b_{r,IF}^C - b_{r,IF}^G$ is a sum of real GPS-Compass system time and a biased term $b_{r,IF}^C - b_{r,IF}^G$. Then Compass observations can be written as:

$$\begin{aligned} \Delta p_{r,j}^C &= -\boldsymbol{\mu}_r^C \cdot \Delta r + m_r^C \cdot \tau_r + dt_r^{G,b} + dt_{sys}^b + \varepsilon_P \\ \Delta \phi_{r,j}^C &= -\boldsymbol{\mu}_r^C \cdot \Delta r + m_r^C \cdot \tau_r + dt_r^{G,b} + dt_{sys}^b + \lambda_j^C \cdot M_{r,j}^{C,b} + \varepsilon_\phi \end{aligned} \tag{33.11}$$

dt_{sys}^b is the estimable GPS-Compass system time difference. The observation equations and unknown vector can be formed:

$$\underset{4m\times 1}{y} = \underset{4m\times(3m+6)}{A} \cdot \underset{(3m+6)\times 1}{x} + \underset{4m\times 1}{\varepsilon_y},\ \varepsilon_y \sim N(0, Q_{yy}) \tag{33.12}$$

$$x = [\Delta r_r, \tau_r, dt_r^b, dt_{sys}^b, I_{r,1}^{s,b}, M_r^{s,b}]^T \tag{33.13}$$

33.2.3 Dynamic Model

The Extended Kalman Filter (EKF) is utilized in the parameter estimation, and the corresponding dynamic model can be denoted as:

$$x(i+1) = \Phi_{i+1,i} \cdot x(i) + \omega(i),\ \omega \sim N(0, Q_{\omega\omega}) \tag{33.14}$$

$\Phi_{i+1,i}$ is the corresponding transition matrix, ω is the normally-distributed process noise with zero-mean and variance–covariance (VC) matrix $Q_{\omega\omega}$.

In dual-frequency PPP, the matrix $\Phi_{i+1,i}$ and $Q_{\omega\omega}$ can be denoted as:

$$\Phi_{i+1,i} = diag\{\underset{3\times3}{I}, 1, 0, \underset{m\times m}{I}, \underset{2m\times 2m}{I}\} \tag{33.15}$$

$$Q_{\omega\omega} = diag\{q_p \cdot \Delta t, q_z \cdot \Delta t, q_t \cdot \Delta t, \underset{m\times m}{q_I} \cdot \Delta t, \underset{2m\times 2m}{0}\} \tag{33.16}$$

where Δt is the time interval between adjacent epochs. The five sub-matrices in $\Phi_{i+1,i}$ correspond to the transition matrices of the positioning, ZTD, receiver clock error, ionospheric delays at L_1 and ambiguities; their corresponding spectral density matrices q_z, q_t and 0 indicate that these four kinds of parameters are modeled as a random walk process, white noise process, random walk process and time-invariant parameter set, respectively. The actual values of elements in the spectral density matrix depend mainly on the practical.

In the dynamic model of dual-frequency combined PPP, an additional parameter dt^b_{sys} is added in the parameter vector, with a transition matrix of identity and modeling as a time-invariant parameter.

33.3 PPP Solutions and Analysis

33.3.1 Data and Models

In this section, a comparative analysis of GPS and Compass PPP was conducted to validate the performance of Compass PPP. Three days datasets of two continuous tracking stations, named as CUT0 and CUTA, were adopted from Curtin University, Australia. The two stations were equipped with Trimble NetR9 receivers, which can track all available GNSS satellites at each open frequency, including GPS (L1, L2, and L5), GLONASS (L1, L2, and L3), Compass (B1, B2, and B3), Galileo (E1, E5a, E5b, and E5a + b) and QZSS (L1, L2, L5, and LEX) satellites. Since the two stations are near, only the results from CUT0 station are showed in this paper.

Figure 33.1 shows the sky plots of GPS and Compass constellations observed at CUT0 (32.00°S, 115.89°E) on March 20, 2012, with a cut-off elevation of 10°. For Compass system, it can be seen that four GEO satellites are stationary and always visible in the northern hemisphere, and five IGSO satellites have a track of 8-sharp. Figure 33.2 shows the visible satellites and PDOP values of GPS-only, Compass-only and combined GPS and Compass constellations at CUT0. The average number of visible satellites for Compass and combined GPS and Compass system are 7.8 and 16.5, with an increase of about 112 %. It can also be seen that there is an obvious decrease of PDOP values when Compass is added to GPS, from the average of 2.94 to 1.38. This will enhance the precision and liability of navigation service using combined GPS and Compass system.

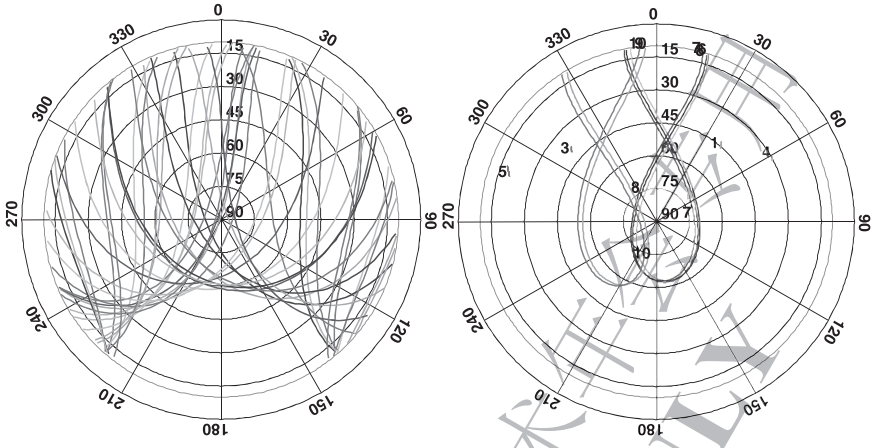

Fig. 33.1 Sky plot (azimuth vs. elevation) of GPS (*left*) and Compass (*right*) at CUT0 on March 20, 2012, cut-off = 10°

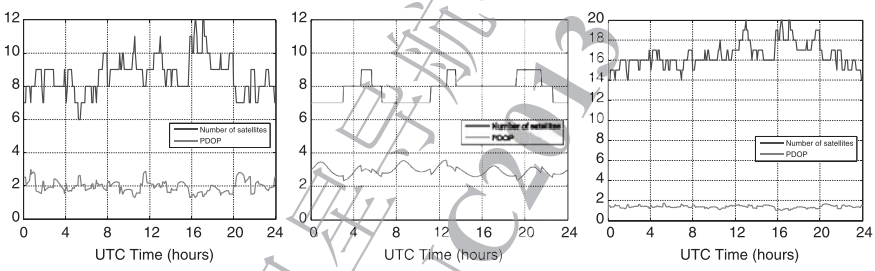

Fig. 33.2 Satellite visibility and PDOP of GPS (*left*), Compass (*middle*) and combined GPS and Compass (*right*) constellations at CUT0 on March 20, 2012, cut-off = 10°

Dual-frequency GPS and Compass observations during March 20th and 22th (DOY 80-82) 2012 are selected for PPP experiments. The Compass orbit and clock products are provided by TUM [15] in current International Terrestrial Reference Frame (ITRF) at an interval of 30 s, which is computed based on 6 Compass-capable receivers distributed in Asia–Pacific area. IGS final orbit and clock products at an interval of 15 min and 30 s, as well as the differential code bias products are used for GPS satellite corrections. For all PPP solution, a cut-off elevation of 10° is adopted and UNB3m model and Global Mapping Function (GMF) are utilized for priori correction of tropospheric delay and mapping function of ZTD estimation. The filter convergence time is defined when the positioning accuracy of each component is better than 10 cm. The reference coordinates for CUT0 and CUTA station are obtained by network adjustment using Bernese 5.0 software, with an accuracy of 3 mm for horizon and 5 mm for vertical.

33.3.2 Dual-Frequency PPP

Compass B1 and B2 frequency observations for three days are utilized for static Compass-PPP. The positioning results are shown in Fig. 33.3, together with the statistics of results after convergence in Table 33.1.

From Fig. 33.3 and Table 33.1, it can be concluded that, based on the existing Compass products from TUM, the positioning results of 1–3 cm can be achieved in dual-frequency Compass-PPP. After filter convergence, the 3D positioning accuracy is better than 3 cm; and the stability of filter can be achieved at a level of 1–2 cm.

The corresponding dual-frequency GPS-PPP results and the statistics are showed in Fig. 33.4 and Table 33.2 respectively. As we know, PPP solutions are sensitive to satellite orbit and clock products. Currently, the Compass orbit and clock products from TUM have a lower accuracy than GPS products from IGS. Therefore, the convergence time of Compass-PPP is longer than GPS-PPP. After filter convergence, the positioning accuracy of Compass-PPP is comparative to GPS-PPP, both at a level of cm.

Figure 33.5 shows the difference of zenith tropospheric delays (ZTD) and receiver clock error estimations from GPS-only and Compass-only PPP. The difference of ZTD is less than 2 cm, with a bias of 0.8 cm and standard deviation of 1.0 cm. Based on Eq. (33.5), the difference of receiver clock estimations can be expressed as:

$$\left(dt_r^b\right)_C - \left(dt_r^b\right)_G = dt_{sys} + b_{r,IF}^C - b_{r,IF}^G \tag{33.17}$$

From Eq. (33.17), it is obvious that above term is same as the estimable biased GPS-Compass time difference dt_{sys}^b, which can be regarded as a constant in daily data; Fig. 33.5 shows that the difference of receiver clock error tends to 571.3–571.5 m, with a standard deviation of 0.1 m.

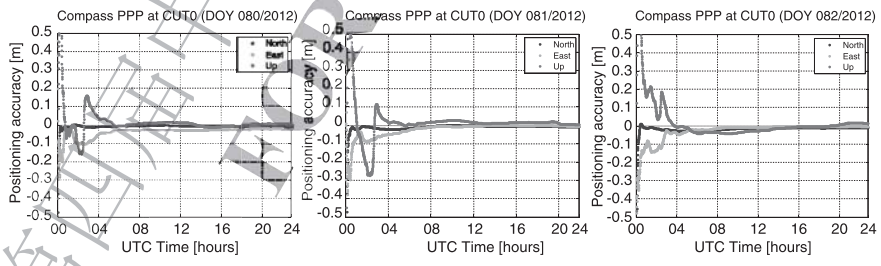

Fig. 33.3 Dual-frequency Compass-PPP positioning results for three days at CUT0

Table 33.1 Statistics of Compass-PPP solutions after convergence at CUT0, in cm

Component	DOY80			DOY81			DOY82		
	Bias	STD	RMS	Bias	STD	RMS	Bias	STD	RMS
North	−0.5	0.2	0.5	−0.6	0.6	0.9	−1.5	0.6	1.6
East	−2.7	0.6	2.8	−0.8	1.3	1.5	−1.0	1.0	1.4
Up	0.5	1.1	1.2	1.5	0.7	1.7	−1.5	1.8	2.4

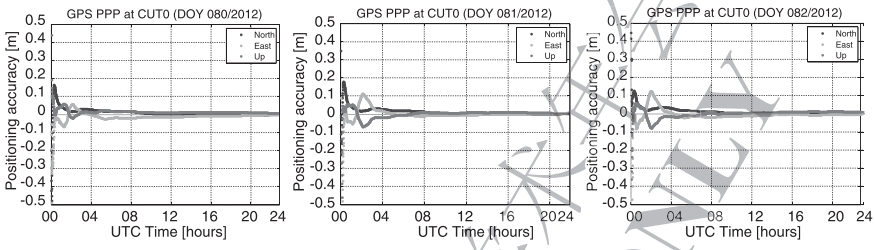

Fig. 33.4 Dual-frequency GPS-PPP positioning results for three days at CUT0

Table 33.2 Statistics of GPS-PPP solutions after convergence at CUT0, in cm

Component	DOY80			DOY81			DOY82		
	Bias	STD	RMS	Bias	STD	RMS	Bias	STD	RMS
North	0.7	0.8	1.1	0.6	0.8	1.0	0.6	0.7	0.9
East	−1.0	0.6	1.2	−0.2	0.5	0.6	−0.9	0.6	1.1
Up	1.3	0.3	1.4	0.5	0.7	0.9	0.5	0.8	0.9

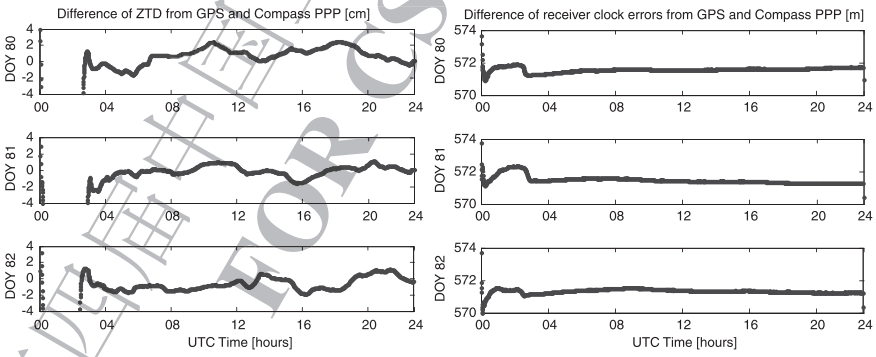

Fig. 33.5 Difference of ZTD (*left*) and receiver clock error (*right*) estimations from GPS and Compass PPP

33.3.3 Dual-Frequency Combined PPP

To evaluate the PPP performance using single and combined GNSS systems, GPS and Compass observations are integrated to perform combined PPP. The initial STD values for GPS and Compass code and phase observations are vital important to define the measure precision of code and phase, as well as their relative precision, a proper weight ratio between GPS and Compass observations can shorten the convergence time and improve the filter stability. Figure 33.6 shows positioning mean and STD of the combined PPP with different STD ratios, where ratio $= \mathrm{STD_C}/\mathrm{STD_G}$.

Figure 33.6 shows that when we give an equal weight for GPS and Compass observations, the stability and accuracy of positioning results will achieve 2–4 and 3.5–4.5 cm respectively, and the optimal STD ratio for Compass/GPS observations is 2.2. Figure 33.7 shows the combined PPP results on DOY080 and 081/2012 with a weight ratio of 2.2. The results show that, combined GPS + Compass PPP can also achieve a positioning accuracy of cm level, and it can shorten the convergence time, from 33 to 30 min, but not necessarily improve positioning results by much if the satellites of the single GNSS system already have good receiver-satellite geometry.

The local overall model (LOM) test analyses the discrepancy between data and given model by means of least squares residual vector $\hat{e}$, with an average of 1 [12]. Where $LOM = \hat{e}^T Q^{-1} \hat{e} / red$, when applying the LOM test in EKF, $\hat{e}$ is the predicted residual, Q is the predicted covariance matrix, and *red* represents the redundancy at the current epoch. Figure 33.8 shows the LOM test statistics accompanying PPP results for Compass and GPS respectively. The repeatability of LOM test for Compass PPP due to the multipath effect.

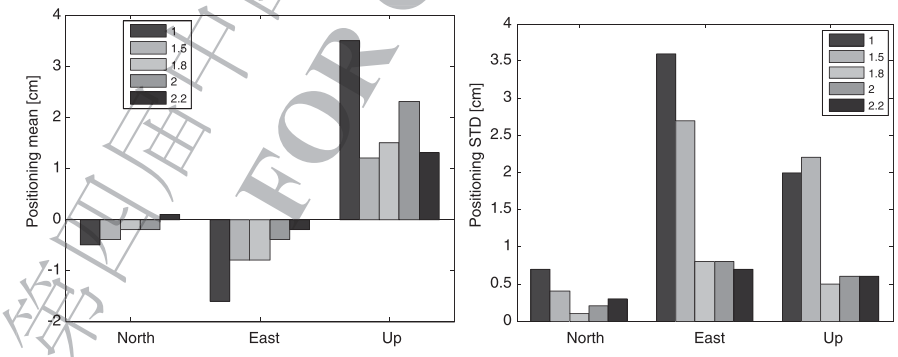

Fig. 33.6 Positioning mean and STD of combined PPP with different STD ratios for Compass/GPS observations

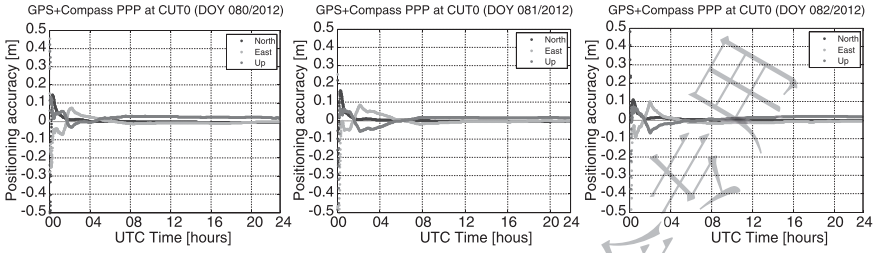

Fig. 33.7 Combined GPS + Compass PPP positioning results for two days at CUT0, STD ratio = 2.2

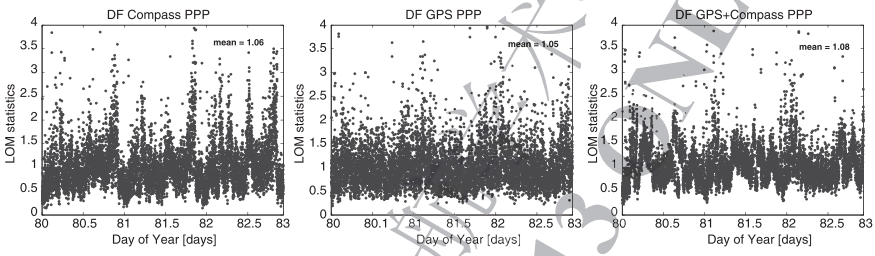

Fig. 33.8 LOM values for Compass, GPS and combined PPP, DOY80-82/2012

33.4 Conclusions

This study reports the performance of dual-frequency Compass-PPP and combined GPS + Compass in static mode in comparison with GPS-PPP. Based on the Compass products from TUM, three daily datasets have been used in the numerical analysis. The main conclusions are as followed:

1) Currently, dual-frequency Compass-PPP is capable of providing static positioning at centimeter level, which is comparative to GPS-PPP.
2) Combined GPS + Compass PPP shorten the convergence time slightly, but it contributes only marginally to the GNSS-only positioning accuracy.

It should be noted that the Compass orbit and clock products from TUM are only based on six stations, and have a lower accuracy than IGS products, which result in the longer time for convergence and less positioning accuracy of Compass-PPP. In future, with more accuracy of Compass products, the positioning accuracy of Compass-PPP will be further improved. Furthermore, PPP technique using Compass triple-frequency signals also needs for attention.

Acknowledgments Thanks to Technology University of Munich (TUM) and German Aerospace Center (DLR) for providing the Compass orbit and clock products. Thanks to Dr. Andrea Nardo from Curtin University for providing the reference coordinates of CUT0 and CUTA stations. This work was jointly supported by National Key Program 863(Grant No. 2011AA120503), National

Key Technology R&D Program (Grant No. 2012BAB16B01), the Fundamental Research Funds for the Central Universities (Grant No. 201121402020009) and Key Laboratory of Geospace Environment & Geodesy Ministry of Education project (Grant No.11-01-08) for financial support.

References

1. Cao C, Jing G, Luo M (2008) COMPASS satellite navigation system development. PNT challenges and opportunities symposium, Stanford, California, USA, 5–6 Nov 2008
2. Cao W, O'Keefe K, Cannon ME (2008) Evaluation of COMPASS ambiguity resolution performance using geometric-based techniques with comparison to GPS and Galileo. ION GNSS 2008, Session B4, Savannah, Georgia, USA, 16–19 Sept 2008
3. Chen HC, Huang YS, Chiang KW, Yang M, Rau RJ (2009) The performance comparison between GPS and BeiDou-2/COMPASS: a perspective from Asia. J Chin Inst Eng 32(5):679–689
4. Chen J, Wu B, Hu X, Zhou S, Cao Y, Wu X, Xing N (2012) Compass/Beidou: system status and initial service; IGS workshop on GNSS Biases, University of Bern, Switzerland, 18–19 Jan 2012
5. Dach R, Brockman E, Schaer S et al (2009) GNSS processing at CODE: status report. J Geodesy 83:353–365. doi:10.1007/s00190-008-0281-2
6. Dow J, Neilan R, Rizos C (2009) The international GNSS service in a changing landscape of global navigation satellite systems. J Geodesy 83:191–198. doi:10.1007/s00190-008-0300-3
7. Kouba J, Héroux H (2001) Precise point positioning using IGS orbit and clock products. GPS Solutions 5(2):12–28
8. Montenbruck O, Hauschild A, Steigenberger P, Hugentobler U, Riley S (2012) A COMPASS for Asia: first experience with the BeiDou-2 regional navigation system. IGS Workshop 2012, Olsztyn, 23–27 July 2012
9. Montenbruck O, Hauschild A, Steigenberger P, Hugentobler U, Teunissen PJG, Nakamura S (2012) Initial assessment of the COMPASS/BeiDou-2 regional navigation satellite system. GPS Solutions. doi:10.1007/s10291-012-0272-x
10. Nadarajah N, Teunissen PJG, Buist P and Steigenberger P (2012) First results of instantaneous GPS/Galileo/COMPASS attitude determination. In: Proceedings of the 6th ESA workshop on satellite navigation user equipment technologies (NAVITEC'12)
11. Nadarajah N, Teunissen PJG and Raziq N (2012) Instantaneous COMPASS-GPS attitude determination: a robustness analysis. Advances in Space Research (submitted)
12. Teunissen PJG (1990) Quality control in integrated navigation systems. IEEE Aerosp Electron Syst Mag 5(7):35–41
13. Shi C, Zhao QL, Li M, Tang WM, Hu ZG, Lou YD, Zhang HP, Niu XJ, Liu JN (2012) Precise orbit determination of Beidou satellites with precise positioning. Sci China Earth Sci 55(7):1079–1086
14. Shi C, Zhao QL, Hu ZG, Liu JN (2012) Precise relative positioning using real tracking data from COMPASS GEO and IGSO satellites. GPS Solutions. doi:10.1007/s10291-012-0264-x
15. Steigenberger P, Montenbruck O, Hauschild A, Hugentobler U (2012) Performance analysis of compass orbit and clock determination and compass-only PPP. IGS Workshop 2012, Olsztyn, 23–27 July 2012
16. Yang YX, Li JL, Xu JY, Tang J, Guo HR, He HB (2011) Contribution of the Compass satellite navigation system to global PNT users. Chin Sci Bull 56(26):2813–2819. doi:10.1007/s11434-011-4627-4
17. Zumberge J, Heflin M, Jefferson D, Watkins M, Webb F (1997) Precise point positioning for the efficient and robust analysis of GPS data from large networks. J Geophys Res 102(B3):5005–5017